

# Deciphering the role of the hendecad-repeat coiled-coil domain of TRIM72 in membrane curvature recognition

Hyun Kyu Song

[hksong@korea.ac.kr](mailto:hksong@korea.ac.kr)

Korea University <https://orcid.org/0000-0001-5684-4059>

Si Hoon Park

Korea University

---

## Article

**Keywords:** coiled-coil, hendecad repeat, membrane curvature, MG53, TRIM72

**Posted Date:** April 25th, 2024

**DOI:** <https://doi.org/10.21203/rs.3.rs-4235080/v1>

**License:**  This work is licensed under a Creative Commons Attribution 4.0 International License.

[Read Full License](#)

**Additional Declarations:** (Not answered)

---

# Abstract

RING-type E3 ubiquitin ligases are functional multidomain proteins involved in diverse eukaryotic cellular processes. A major subfamily of RING-type ligases is the tripartite motif (TRIM)-containing protein family, whose members contain RING, B-box, coiled-coil, and variable C-terminal domains. Although the roles of individual TRIM domains are well understood, the function of the coiled-coil domain remains unclear owing to its structural complexity. In this study, we investigated the structural details of the coiled-coil domain of TRIM72 to elucidate its role in facilitating interactions with both concave and convex membranes. Cooperative interactions of the coiled-coil/coiled-coil and B-box/B-box domains were found to drive oligomerization, aiding in the recognition of phospholipid layers by the PRYSPRY domains. These insights provide a fundamental basis for understanding TRIM family E3 ligases and highlight their conserved molecular architecture and pattern recognition capabilities through higher-order assembly.

## INTRODUCTION

E3 ubiquitin (Ub) ligases play critical roles in target selection for degradation and can trigger signal transduction, membrane trafficking, DNA damage repair, and membrane repair<sup>1,2</sup>. They are classified into three different types depending on the mechanism of Ub transfer: the Really Interesting New Gene (RING), Homologous to E6-AP Carboxyl Terminus (HECT), and RING-Between-RING (RBR) Ub ligases<sup>3,4</sup>. Among these classes, RING is dominant, and one of the most abundant families of RING-type Ub ligases comprise the TRIpartite Motif (TRIM)-containing proteins, which contains more than 80 members among the 600 Ub ligases found in humans<sup>5,6</sup>.

Members of the TRIM superfamily contain multimodular domains<sup>7</sup>, including relatively conserved N-terminal RBCC (RING, B-box, and coiled-coil) and variable C-terminal domains (Fig. 1a). Although they have a similar architecture, their functions are diverse and involve many cellular processes, such as retroviral restriction (TRIM5, TRIM22, and TRIM25)<sup>8,9,10,11</sup>, DNA damage response (TRIM24)<sup>12</sup>, gene silencing (TRIM28 and TRIM71)<sup>13,14</sup>, autophagy (TRIM32)<sup>15</sup>, and membrane repair (TRIM72)<sup>2</sup>. As diverse as their roles, mutations in TRIM genes cause various genetic disorders, including Mulibrey Nanism (TRIM37)<sup>16</sup>, Sjögren's syndrome (TRIM21/Ro52)<sup>17,18,19,20</sup>, Opitz G/BBB syndrome (TRIM18/MID1)<sup>21,22</sup>, familial Mediterranean fever (TRIM20/pyrin)<sup>23</sup>, acute promyelocytic leukemia (TRIM19/PML)<sup>24</sup>, and muscular dystrophy (TRIM32)<sup>25</sup>. Despite the increasing number of genetic and cellular studies, biochemical and structural evidence are still limited, and only domain structures are available<sup>26,27,28,29,30,31,32</sup>. We recently presented dimeric and oligomeric structures of TRIM72, in which oligomerization was found to be coupled to ubiquitylation and phospholipid membrane recognition<sup>33</sup>.

TRIM72, also known as mitsugumin 53 (MG53), is expressed mainly in muscles<sup>34,35,36</sup> and is a key initiator of the plasma membrane repair machinery following acute membrane damage, such as that induced by ischemia/reperfusion injury<sup>2,37,38</sup>. Furthermore, recombinant TRIM72 has shown therapeutic

potential for a variety of muscle and non-muscle tissue injuries<sup>36</sup>. In previous studies, the oligomerization of TRIM72 was shown to be a key process for membrane repair and activation<sup>31,33</sup>. TRIM72 facilitates negatively charged small repair vesicles to injury sites on the plasma membrane. The TRIM72-bound repair vesicles are assumed to accumulate at the injury site where they form a membrane patch to seal holes in the plasma membrane<sup>33,39</sup>. In addition to membrane repair, TRIM72 participates in diverse cellular processes that occur in the membrane environment, such as filopodia-like structures, exocytosis, caveolar structures, and lipid rafts<sup>34,40,41</sup>. It is unknown whether the TRIM72 oligomer can sense or induce specific features of membrane formation, such as convex or concave surfaces. Therefore, this study aimed to comprehensively analyze the coiled-coil structure of TRIM72 and to visualize TRIM72-bound liposomes using cryo-transmission electron microscopy (cryo-TEM). The results indicated that TRIM72 can sense any type of membrane curvature to induce membrane patch formation via self-oligomerization.

## MATERIALS AND METHODS

### Small-angle X-ray scattering

Details of sample preparation, data collection, and parameters for the SAXS experiments used have been described in a previous report<sup>33</sup>. *Ab initio* structure determination was performed using DAMMIN software in ATSAS online (<https://www.embl-hamburg.de/biosaxs/atsas-online/>). The DAMMIN models evaluated using DAMSEL were superimposed using DAMSUP and averaged through DAMAVER<sup>42</sup>. The averaged SAXS envelope models were superimposed with the crystallographic model of *m*TRIM72 ΔRING by using SUPCOMB in the ATSAS software package<sup>43</sup>. Detailed parameters and results are described in **Supplementary Table 1**.

### Cryo-TEM

Details of sample preparation and cryo-TEM data collection methods used have been described in a previous report<sup>33</sup>. For cryo-experiments, protein-80 mol% PS-SUV complexes were loaded onto glow-discharged Quantifoil grids and frozen in a plunge freezer with a Vitrobot (Thermo Fisher Scientific, Waltham, MA, USA). Cryo-TEM images were collected at the Korea Basic Science Institute (Daejeon, South Korea) using a Titan Krios transmission electron microscope (Thermo Fisher Scientific) operated at 300 kV and recorded with a Falcon 3EC direct electron detector (Thermo Fisher Scientific).

### Multiple sequence and structure analyses

#### Coi

Coiled-coil sequences from human TRIM family proteins were aligned via Clustal<sup>44</sup> and further analyzed using BioEdit software<sup>45</sup>. A logo graph was generated using WebLogo (<https://weblogo.berkeley.edu/logo.cgi>). Structural analyses were performed using the PISA server in the

CCP4 suite<sup>46</sup>. Structure-based sequence alignment was conducted using PROMALS3D<sup>47</sup>, with minor modifications.

## Structure display and presentation

All structural figures were prepared with *PyMOL* (Schrödinger, LLC, New York, NY, USA). The membrane model in Fig. 1b was generated from a POPS/POPC bilayer<sup>48</sup>.

## RESULTS

### Overall structure of TRIM72 with an unusual coiled-coil domain

TRIM72 adopts the domain organization standard of TRIM proteins: an RBCC domain followed by a unique PRYSPRY domain (class IV), which is the largest among the 11 TRIM protein subgroups (Fig. 1a). Previously, we prepared wild-type mouse TRIM72 using a bacterial expression system and determined its structure using X-ray crystallography<sup>33</sup>. Tight dimeric TRIM72 is shaped like a bird with wide wings (Fig. 1b). The coiled-coil, like outstretched wings, forms an antiparallel dimer with a length of approximately 170 Å. The core structure consists of H1:H1' helices, heptad H3:H3' helices (prime indicates the second protomer of the dimer), and a pair of PRYSPRY domains that are structurally rigid in our dimer models, a feature unique to the TRIM superfamily<sup>49,50,51,52</sup>. Dozens of polar and nonpolar bonds are present at the dimeric interface, which has a total buried surface of ~ 5,000 Å<sup>2</sup>. Our previous biochemical results confirmed that the PRYSPRY domain launches on the membrane surface and is mediated by interactions between the positively charged residues of PRYSPRY and phosphatidylserine (PS) lipids of the membrane<sup>33</sup>.

### Flexible nature of the RBCC domain

In our crystal structure, the zinc-bound RING domains at each N-terminus of TRIM72 exist in a closed conformation and interact with the coiled-coil of the other protomer (Fig. 1b), which may block access to E2-Ub conjugates for Ub transfer. To determine whether the RING domain also adopts a closed conformation in solution, we performed small-angle X-ray scattering (SAXS) analysis with full-length TRIM72 and a deletion construct of the RING domain ( $\Delta$ RING) (Fig. 2a). The crystal structures were fitted to SAXS molecular envelopes, showing the flexible nature of the peripheral region of TRIM72, particularly the RING domain (Fig. 2b). Therefore, we concluded that the closed conformation of the RING domain was visible owing to molecular contact with the coiled-coil in the crystal structure. As shown in the SAXS model, the RING appeared to be highly mobile and was not visible in the electron density map of most full-length crystal forms<sup>33</sup>. Furthermore, the B-box domain located at the end of the coiled-coil was mobile. In our structures, as well as in the cryo-TEM and crystal structures from other research groups<sup>31,32,33</sup>, the RING, B-box domain, and part of the coiled-coil showed no or very weak densities for chain tracing, suggesting that these peripheral parts of TRIM72 are highly dynamic. When we

superimposed our TRIM72 crystal structures, it was evident that the core region comprising two PRYSPRY and nearby H1:H1' coiled-coil domains was highly rigid (Fig. 2c). Interestingly, large structural changes were found at each end of the coiled-coil, which moved only “up and down” and not from “side to side” (Fig. 2c). From the well-matched hendecad repeats to the flexible ends of the coiled-coil, the change in conformation gradually increases and moves the protein up to ~ 20 Å (Fig. 2d).

## Comparison of coiled-coil domains among TRIM-family proteins

To investigate whether this “up and down” flapping motion of the coiled-coil is preserved in the TRIM superfamily, we compared the structures in all available TRIM coiled-coil domains (mouse TRIM72, monkey TRIM5a, human TRIM20, human TRIM25, human TRIM28, and human TRIM69)<sup>49,50,51,52,53</sup> (Fig. 3). The TRIM coiled-coil domains showed a unique pattern comprising a mixture of heptad and hendecad repeats: trimeric heptad, dimeric heptad, and dimeric hendecad interfaces (Fig. 3). All structure-determined coiled-coil domains showed similar heptad (*a-g*) and hendecad (*a-k*) repeats, although there were some deviations observed in the heptad repeats in H2 and H3 helices (Fig. 3a). The buried positions of the heptad and hendecad repeats are well aligned in the H1 helix (Fig. 3b). The superimposition showed a similar “up and down” motion of coiled-coil domains as that found in TRIM72 (Fig. 3c).

We explored other TRIM superfamily proteins using multiple sequence alignments. The 64 human TRIM coiled-coil domains showed conserved repeats at hydrophobic positions (**Supplementary Fig. 1**). The most extended H1 helix comprises heptad and hendecad repeats. The dimeric coiled-coil heptads are formed by the interaction between H1 and H1' helices, and the trimeric heptads by the interactions among H1, H1', and H2' helices (Fig. 4a). The interfaces were divided into four regions: trimeric heptad, dimeric heptad, dimeric hendecad, and tetrameric hendecad/heptad interfaces (Fig. 4a). The overall conservation of hydrophobic residues was well aligned in the coiled-coil of TRIM proteins. For example, hydrophobic positions are ordered in the trimeric heptads and dimeric hendecads of the H1 helix to form dimeric and trimeric interactions (**Supplementary Fig. 2**). Interestingly, we found that the *a* and *d* positions of the first dimeric heptads in the H1 helix showed relatively hydrophilic properties, although all were buried in the crystal structures (Fig. 3b). As shown in Fig. 2d, the root-mean-square deviation (r.m.s.d.) among the TRIM72 structures also increased gradually at residue number 150 toward the N-terminal peripheral region of the coiled-coil. This supports that the hydrophilic buried positions at the dimeric heptad interface might induce flapping of the coiled-coil in the TRIM superfamily.

## Helix packing of the four helical bundle

The dimeric hendecad repeats in the H1 helix were the most rigid part shown in the r.m.s.d. analysis among all determined TRIM72 structures (Fig. 2c,d), as well as in comparison with the structurally characterized TRIM coiled-coil domains (Fig. 3c). This region was the most conserved among the 64 human TRIM family proteins (**Supplementary Fig. 2**). However, the core hendecad region of TRIM72

forms a unique tetrameric hendecad/heptad helix packing structure compared to that of other TRIM proteins (Fig. 4b-g). The H3 helix forms an antiparallel dimer with the H3' helix of the other protomer and further packs against four-helical bundles at the middle of the antiparallel H1:H1' dimer (Fig. 5a). A tetrahelical bundle consisting of the H3:H3' heptad and H1:H1' hendecad dimers at an angle of 50°, which is commonly observed for  $\alpha$ -helix packing<sup>54</sup>, is present, although the corresponding bundles in other TRIM coiled-coils showed different angles (Fig. 4c-g). The stable four-helical bundle structure of TRIM72 is critical for its function, as confirmed by the deletion of the H3 helix, which lacks a membrane-binding affinity<sup>33</sup>. The angles between hendecad H1:H1' and heptad H3:H3' are variable from 0 to 90° among the TRIM-family proteins (Fig. 4b-g). As shown in the domain architecture of TRIM-family proteins, additional functional domains exist after the H3 helix. Therefore, orientation of the H3:H3' heptad might be important for the physiological role of TRIM-family proteins.

With the rigid core tetrahelical bundle structure, the C-terminal PRYSPRY domains, acting like the “bird’s body,” are located on the opposite side of the middle of the coiled-coil across the dimer comprising H3:H3' helices (Fig. 1b). A pair of PRYSPRY domains are completely separated at a distance of approximately 10 Å, but interestingly, each domain possesses positively charged surfaces on the same side opposite the coiled-coil (Fig. 1b). In the PRYSPRY domains, many arginine (R356, R368, R369, R371, and R386) and lysine residues (K317, K330, K389, K398, K460, and K462) protrude toward the bottom of the “bird’s body,” much like “claws” (Fig. 1b). Orientation of the two aligned PRYSPRY domains is tightly maintained by H3:H3' helix interactions. Considering the two aligned PRYSPRY domains, a unique structural feature of TRIM72 is that it binds to PS to recognize vesicular and plasma membranes<sup>2,33</sup>.

## Optimized architecture for recognizing both positive and negative curvatures of the membrane

We previously examined microvesicles using electron microscopy (EM)<sup>33</sup>. As shown by the negative EM, the TRIM72 fractions coexisted with microsomes that were approximately 100 µm in size, and the TRIM72 oligomer laid on the membrane in tandem. This striped pattern was also observed for the reconstituted TRIM72-liposomes *in vitro*. To obtain a model of the oligomer in its native state at a higher resolution, we visualized the higher-order TRIM72 assembly on the membrane using cryo-TEM (Fig. 6a). TRIM72 molecules bound to PS-liposomes were clearly visible. Moreover, TRIM72/TRIM72 contacts across separate liposomes were observed. The two-sided membrane-bound oligomer model also accounted for the higher-order assembly found in the space between the two membrane surfaces, as shown in the cryo-TEM images (Fig. 6a). When facing opposite sides, the aligned PRYSPRY domains can recognize both separated membranes. Furthermore, the distance between each opposite PRYSPRY domain was approximately 11 nm, which was almost the same as the gap observed between membrane surfaces with a higher-order assembly. Therefore, we concluded that TRIM72 likely accumulates in lipid membranes during patch formation via self-oligomerization.

In addition to this higher-order assembly observed in the spaces between liposomes, we found a TRIM72 assembly on both the convex and concave surfaces of liposomes (Fig. 6b,c). The unique architecture of

TRIM72 allows its promiscuous interaction with any membrane shape if the membrane is enriched with PS. Indeed, TRIM72 molecules have been reported to exist in structures with positively curved membranes, such as caveolae<sup>34,55</sup> and negatively curved membranes, such as filopodia-like structures<sup>41</sup>. Using cryo-electron tomography (ET), we previously reconstructed the three-dimensional structure of higher-order-assembled TRIM72 on large, almost flat liposomes<sup>33</sup>. The elongated architecture of the TRIM72 oligomer and connections between TRIM72 molecules were visible, and the TRIM72 oligomer clearly separated from the phospholipid layer in the raw tomograms (Fig. 3b, c).

## DISCUSSION

The bird-like shape of the dimeric TRIM72 is optimal for its function. The wing-shaped coiled-coil domain exhibited flexible movement only in the up-and-down direction, and the dynamic nature of this movement gradually increased toward the end of the wings and was linked to the RING domain (Fig. 2).

Intermolecular interactions between the B-boxes located at the ends of the wings are critical for the higher-order assembly of TRIM72. The RING domain is extremely flexible in regulating the inactive-active transition via intermolecular dimerization on PS-enriched membranes<sup>33</sup>. Membrane binding is a prerequisite for oligomerization, which activates TRIM72 ubiquitylation. Three separate modules for the interaction between PRYSPRY domains and the membrane work in harmony: the flexible bending motion of the coiled-coil, the higher-order assembly by B-box/B-box domain interactions, and the highly dynamic nature of the RING domain. These structural features of TRIM72 are likely critical for its membrane repair function (Fig. 7).

In this study, we presented structural details of the TRIM72 coiled-coil for liposome-binding properties through oligomerization. Structural analysis revealed that the dimeric heptads in the H1 helix and four-helical bundle at the center of the coiled-coil exhibited the highest flexibility and rigidity, respectively. In the dimeric heptads, hydrophilic residues are buried at the interface, which is a unique feature of TRIM coiled-coil domains, whereas hydrophobic residues are exposed on the surface, which is crucial for TRIM72 oligomerization and subsequent membrane binding<sup>33</sup>. The four-helical bundle also plays a vital role in membrane binding and structural integrity, as it is packed at various angles among the TRIM family. Interestingly, recent crystal structures of TRIM28 RBCC complexed with the CUE1 domain of SMARCAD1 and the KRAB domain of ZNF93 revealed that both dimeric heptads and the four-helical bundle are essential for each interaction mediated by the hydrophobic interface<sup>56,57</sup>. This suggests that these regions could serve as substrate-binding sites for Ub transfer. Indeed, the catalytic RING domain is located close to the dimeric heptad region in our crystal structure, which is consistent with other TRIM28 RBCC structures reported previously<sup>56,57</sup>.

However, the molecular mechanisms underlying membrane repair remain largely unknown. Although calcium influx positively regulates the repair process, TRIM72 facilitates small vesicle formation in a calcium-independent manner, directly recognizing PS-enriched membranes and resisting interference by Ca<sup>2+</sup>-PS interactions through oligomerization<sup>33</sup>. We found that patch formation in the membrane

occurred through the self-oligomerization of TRIM72. Due to the absence of a molecular model, it is unclear how TRIM72 mediates patch formation. Based on the average distance between patched vesicles and subtomogram average of the higher-order TRIM72 assembly, we suggested that intermolecular interactions between coiled-coil domains might play a pivotal role in the second round of higher-order assembly for patch formation.

In general, proteins that bind to biological membranes exhibit curvature specificity. Peripheral membrane proteins interact with biological membranes via different mechanisms. One common mechanism involves the formation of amphipathic helices. These are helical segments, with one side being hydrophobic for binding to the lipid core of the membrane and the other side being hydrophilic for surrounding water. When these helices encounter curved membranes, they are inserted into the lipid bilayer in a manner that matches their curvature. Another mechanism involves specific curvature-sensing domains. These domains have the intrinsic ability to recognize and bind to curved membranes. For example, BAR (Bin/Amphiphysin/Rvs; amphiphysin is a brain-enriched protein with an N-terminal lipid interaction) domains are known for their curvature-sensing properties<sup>58</sup>. The BAR domain is banana-shaped and binds to membranes via its concave and convex faces, depending on its class (F-BAR or I-BAR). Furthermore, BAR domains not only sense membranes, but also induce membrane remodeling *in vitro* and *in vivo*. In the current study, we could not observe morphological changes in the liposomes induced by TRIM72; however, this could be determined by investigating extensive physiological conditions in future studies.

TRIM72 interacts with PS-enriched membranes via immunoglobulin-fold PRYSPRY domains, which show robust binding to any type of membrane curvature (Fig. 6). The minimal unit of TRIM72 is a dimer, and the two separated and relatively flat PRYSPRY domains augment lipid binding (Fig. 7). When TRIM72 molecules localize to the membrane, they form a high-order assembly with a regular pattern<sup>33</sup>. More importantly, as visualized via cryo-TEM and cryo-ET (Fig. 6), a higher-order assembly of TRIM72 was formed at both the concave and convex surfaces of the membrane. As shown in our previous subtomogram-averaged model of TRIM72 oligomers, TRIM72 also binds relatively flat membranes<sup>33</sup>. TRIM72 participates in various cellular processes that require membrane dynamics; thus, it can bind to any type of membrane and accumulate PS lipids promiscuously. All TRIM-family proteins share the RBCC motif. In particular, the unusual coiled-coil containing several different repeats, including the hendecad motif, plays a critical role in providing flexibility to the extended structure of TRIM proteins. Indeed, oligomerization is a critical process for members of the TRIM class IV family to biochemically recognize various shapes of curved and patterned platforms, such as phospholipid membranes, viral capsids, and double-stranded nucleic acids, including dsDNA and dsRNA<sup>2,50,59,60</sup>. The functional relationship between higher-order assembly and substrate diversity of other TRIM classes requires further examination in future studies.

## Declarations

# CONFLICT OF INTEREST STATEMENT

The authors declare no competing interests.

## AUTHOR CONTRIBUTIONS

S.H.P. and H.K.S. designed the experiments; S.H.P. performed the SAXS and EM experiments; and S.H.P. and H.K.S. analyzed the data and wrote the manuscript.

## ACKNOWLEDGMENTS

We thank the staff of beamline 4C at the Pohang Accelerator Laboratory, South Korea. We also thank the staff of the cryo-TEM facility at the Korea Basic Science Institute for conducting the cryo-TEM experiment. This study was supported by National Research Foundation of Korea (NRF) grants from the Korean government (Grant Nos. 2020R1A2C3008285, 2020R1A5A1019023, 2021M3A9I4030068, and 2022M3A9G8082638).

## References

1. Komander, D. & Rape, M. The ubiquitin code. *Annual review of biochemistry* 81, 203–229 (2012).
2. Cai C, M.H., Weisleder N, Matsuda N, Nishi M, Hwang M, Ko JK, Lin P, Thornton A, Zhao X, Pan Z, Komazaki S, Brotto M, Takeshima H, Ma J. MG53 nucleates assembly of cell membrane repair machinery. *Nat Cell Biol* 11, 55–64 (2009).
3. Dove, K.K. & Klevit, R.E. RING-between-RING E3 ligases: emerging themes amid the variations. *Journal of molecular biology* 429, 3363–3375 (2017).
4. Zheng, N. & Shabek, N. Ubiquitin Ligases: Structure, Function, and Regulation. *Annu Rev Biochem* 86, 129–157 (2017).
5. Ikeda, K. & Inoue, S. TRIM proteins as RING finger E3 ubiquitin ligases. *Adv Exp Med Biol* 770, 27–37 (2012).
6. Fiorentini, F., Esposito, D. & Rittinger, K. Does it take two to tango? RING domain self-association and activity in TRIM E3 ubiquitin ligases. *Biochemical Society Transactions* 48, 2615–2624 (2020).
7. Meroni, G. & Diez-Roux, G. TRIM/RBCC, a novel class of 'single protein RING finger' E3 ubiquitin ligases. *Bioessays* 27, 1147–1157 (2005).
8. Ganser-Pornillos, B.K. et al. Hexagonal assembly of a restricting TRIM5alpha protein. *Proc Natl Acad Sci U S A* 108, 534–539 (2011).
9. Nisole, S., Stoye, J.P. & Saib, A. TRIM family proteins: retroviral restriction and antiviral defence. *Nat Rev Microbiol* 3, 799–808 (2005).

10. Eldin, P. et al. TRIM22 E3 ubiquitin ligase activity is required to mediate antiviral activity against encephalomyocarditis virus. *J Gen Virol* 90, 536–545 (2009).
11. Koliopoulos, M.G. et al. Molecular mechanism of influenza A NS1-mediated TRIM25 recognition and inhibition. *Nature communications* 9, 1–13 (2018).
12. Jain, A.K., Allton, K., Duncan, A.D. & Barton, M.C. TRIM24 is a p53-induced E3-ubiquitin ligase that undergoes ATM-mediated phosphorylation and autodegradation during DNA damage. *Mol Cell Biol* 34, 2695–2709 (2014).
13. Fasching, L. et al. TRIM28 represses transcription of endogenous retroviruses in neural progenitor cells. *Cell Rep* 10, 20–28 (2015).
14. Welte, T. et al. The RNA hairpin binder TRIM71 modulates alternative splicing by repressing MBNL1. *Genes Dev* 33, 1221–1235 (2019).
15. Di Rienzo, M., Piacentini, M. & Fimia, G.M. A TRIM32-AMBRA1-ULK1 complex initiates the autophagy response in atrophic muscle cells. *Autophagy* 15, 1674–1676 (2019).
16. Kallijarvi, J., Avela, K., Lipsanen-Nyman, M., Ulmanen, I. & Lehesjoki, A.E. The TRIM37 gene encodes a peroxisomal RING-B-box-coiled-coil protein: classification of mulibrey nanism as a new peroxisomal disorder. *Am J Hum Genet* 70, 1215–1228 (2002).
17. Espinosa, A. et al. Loss of the lupus autoantigen Ro52/Trim21 induces tissue inflammation and systemic autoimmunity by disregulating the IL-23-Th17 pathway. *J Exp Med* 206, 1661–1671 (2009).
18. Rhodes DA, T.J. TRIM21 is a trimeric protein that binds IgG Fc via the B30.2 domain. *Mol Immunol* 44, 2406–2414 (2007).
19. Ozato K, S.D., Chang TH, Morse HC 3rd. TRIM family proteins and their emerging roles in innate immunity. *Nat Rev Immunol.* 8, 849–860 (2008).
20. Kong, H.J. et al. Cutting edge: autoantigen Ro52 is an interferon inducible E3 ligase that ubiquitinates IRF-8 and enhances cytokine expression in macrophages. *J Immunol* 179, 26–30 (2007).
21. Berti, C., Fontanella, B., Ferrentino, R. & Meroni, G. Mig12, a novel Opitz syndrome gene product partner, is expressed in the embryonic ventral midline and co-operates with Mid1 to bundle and stabilize microtubules. *BMC Cell Biol* 5, 9 (2004).
22. Trockenbacher, A. et al. MID1, mutated in Opitz syndrome, encodes an ubiquitin ligase that targets phosphatase 2A for degradation. *Nat Genet* 29, 287–294 (2001).
23. Schaner, P. et al. Episodic evolution of pyrin in primates: human mutations recapitulate ancestral amino acid states. *Nat Genet* 27, 318–321 (2001).
24. Wang, P. et al. RING tetramerization is required for nuclear body biogenesis and PML sumoylation. *Nature communications* 9, 1–10 (2018).
25. Kudryashova, E., Kudryashov, D., Kramerova, I. & Spencer, M.J. Trim32 is a ubiquitin ligase mutated in limb girdle muscular dystrophy type 2H that binds to skeletal muscle myosin and ubiquitinates actin.

J Mol Biol 354, 413–424 (2005).

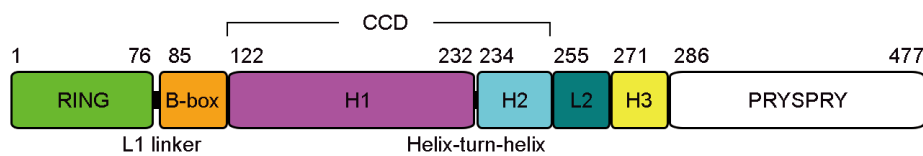
26. Keeble AH, K.Z., Forster A, James LC. TRIM21 is an IgG receptor that is structurally, thermodynamically, and kinetically conserved. Proc Natl Acad Sci 105, 6045–6050 (2008).
27. Masters SL, Y.S., Willson TA, Zhang JG, Palmer KR, Smith BJ, Babon JJ, Nicola NA, Norton RS, Nicholson SE. The SPRY domain of SSB-2 adopts a novel fold that presents conserved Par-4-binding residues. Nat Struct Mol Biol. 13, 77–84 (2006).
28. Kuang Z, Y.S., Xu Y, Lewis RS, Low A, Masters SL, Willson TA, Kolesnik TB, Nicholson SE, Garrett TJ, Norton RS. SPRY domain-containing SOCS box protein 2: crystal structure and residues critical for protein binding. J Mol Biol 386, 662–674 (2009).
29. Grütter C, B.C., Capitani G, Mittl PR, Papin S, Tschopp J, Grütter MG. Structure of the PRYSPRY-domain: implications for autoinflammatory diseases. FEBS Lett 580, 99–106 (2006).
30. Park, E.Y. et al. Crystal structure of PRY-SPRY domain of human TRIM72. Proteins 78, 790–795 (2010).
31. Ma, Y., Ding, L., Li, Z. & Zhou, C. Structural basis for TRIM72 oligomerization during membrane damage repair. Nat Commun 14, 1555 (2023).
32. Niu, Y. et al. Cryo-EM structure of human MG53 homodimer. Biochem J 479, 1909–1916 (2022).
33. Park, S.H. et al. Structure and activation of the RING E3 ubiquitin ligase TRIM72 on the membrane. Nat Struct Mol Biol 30, 1695–1706 (2023).
34. Lee, C.S. et al. TRIM72 negatively regulates myogenesis via targeting insulin receptor substrate-1. Cell Death Differ 17, 1254–1265 (2010).
35. Corona, B.T. et al. Effect of recombinant human MG53 protein on tourniquet-induced ischemia-reperfusion injury in rat muscle. Muscle Nerve 49, 919–921 (2014).
36. He, B. et al. Enhancing muscle membrane repair by gene delivery of MG53 ameliorates muscular dystrophy and heart failure in delta-Sarcoglycan-deficient hamsters. Mol Ther 20, 727–735 (2012).
37. Cao, C.M. et al. MG53 constitutes a primary determinant of cardiac ischemic preconditioning. Circulation 121, 2565–2574 (2010).
38. Duann, P. et al. MG53-mediated cell membrane repair protects against acute kidney injury. Science translational medicine 7, 279ra236-279ra236 (2015).
39. Yi, J. et al. MG53 Preserves Neuromuscular Junction Integrity and Alleviates ALS Disease Progression. Antioxidants (Basel) 10, 1522 (2021).
40. Tan, T., Ko, Y.G. & Ma, J. Dual function of MG53 in membrane repair and insulin signaling. BMB Rep 49, 414–423 (2016).
41. Cai C, M.H., Weisleder N, Pan Z, Nishi M, Komazaki S, Takeshima H, Ma J. MG53 regulates membrane budding and exocytosis in muscle cells. J Biol Chem 284, 3314–3322 (2009).
42. Volkov, V.V. & Svergun, D.I. Uniqueness of ab initio shape determination in small-angle scattering. J Appl Crystallogr 36, 860–864 (2003).

43. Kozin, M.B. & Svergun, D.I. Automated matching of high- and low-resolution structural models. *J Appl Crystallogr* 34, 33–41 (2001).
44. Sievers, F. et al. Fast, scalable generation of high-quality protein multiple sequence alignments using Clustal Omega. *Mol Syst Biol* 7, 539 (2011).
45. Hall, T.A. BioEdit: A User-Friendly Biological Sequence Alignment Editor and Analysis Program for Windows 95/98/NT. *Nucleic Acids Symposium Series* 41, 95–98 (1999).
46. Krissinel, E. & Henrick, K. Inference of macromolecular assemblies from crystalline state. *J Mol Biol* 372, 774–797 (2007).
47. Pei, J., Kim, B.H. & Grishin, N.V. PROMALS3D: a tool for multiple protein sequence and structure alignments. *Nucleic Acids Res* 36, 2295–2300 (2008).
48. Gurtovenko, A.A. & Vattulainen, I. Membrane potential and electrostatics of phospholipid bilayers with asymmetric transmembrane distribution of anionic lipids. *J Phys Chem B* 112, 4629–4634 (2008).
49. Sanchez, J.G. et al. The tripartite motif coiled-coil is an elongated antiparallel hairpin dimer. *Proceedings of the National Academy of Sciences* 111, 2494–2499 (2014).
50. Goldstone, D.C. et al. Structural studies of postentry restriction factors reveal antiparallel dimers that enable avid binding to the HIV-1 capsid lattice. *Proceedings of the National Academy of Sciences* 111, 9609–9614 (2014).
51. Weinert, C., Morger, D., Djekic, A., Grütter, M.G. & Mittl, P.R. Crystal structure of TRIM20 C-terminal coiled-coil/B30.2 fragment: implications for the recognition of higher order oligomers. *Scientific reports* 5, 1–10 (2015).
52. Stoll, G.A. et al. Structure of KAP1 tripartite motif identifies molecular interfaces required for retroelement silencing. *Proceedings of the National Academy of Sciences* 116, 15042–15051 (2019).
53. Li, Y. et al. Structural insights into the TRIM family of ubiquitin E3 ligases. *Cell research* 24, 762–765 (2014).
54. Chothia, C. Principles that determine the structure of proteins. *Annual review of biochemistry* 53, 537–572 (1984).
55. Zhu, H. et al. Polymerase transcriptase release factor (PTRF) anchors MG53 protein to cell injury site for initiation of membrane repair. *J Biol Chem* 286, 12820–12824 (2011).
56. Lim, M. et al. A ubiquitin-binding domain that binds a structural fold distinct from that of ubiquitin. *Structure* 27, 1316–1325. e1316 (2019).
57. Stoll, G.A., Pandiloski, N., Douse, C.H. & Modis, Y. Structure and functional mapping of the KRAB-KAP1 repressor complex. *EMBO J* 41, e111179 (2022).
58. Qualmann, B., Koch, D. & Kessels, M.M. Let's go bananas: revisiting the endocytic BAR code. *EMBO J* 30, 3501–3515 (2011).

59. Kato, K. et al. Structural analysis of RIG-I-like receptors reveals ancient rules of engagement between diverse RNA helicases and TRIM ubiquitin ligases. *Molecular cell* 81, 599–613. e598 (2021).
60. Biris, N. et al. Structure of the rhesus monkey TRIM5alpha PRYSPRY domain, the HIV capsid recognition module. *Proc Natl Acad Sci U S A* 109, 13278–13283 (2012).
61. Shindyalov, I.N. & Bourne, P.E. Protein structure alignment by incremental combinatorial extension (CE) of the optimal path. *Protein Eng* 11, 739–747 (1998).
62. Lek, A. et al. Calpains, cleaved mini-dysferlinC72, and L-type channels underpin calcium-dependent muscle membrane repair. *J Neurosci* 33, 5085–5094 (2013).

## Figures

**a**



**b**

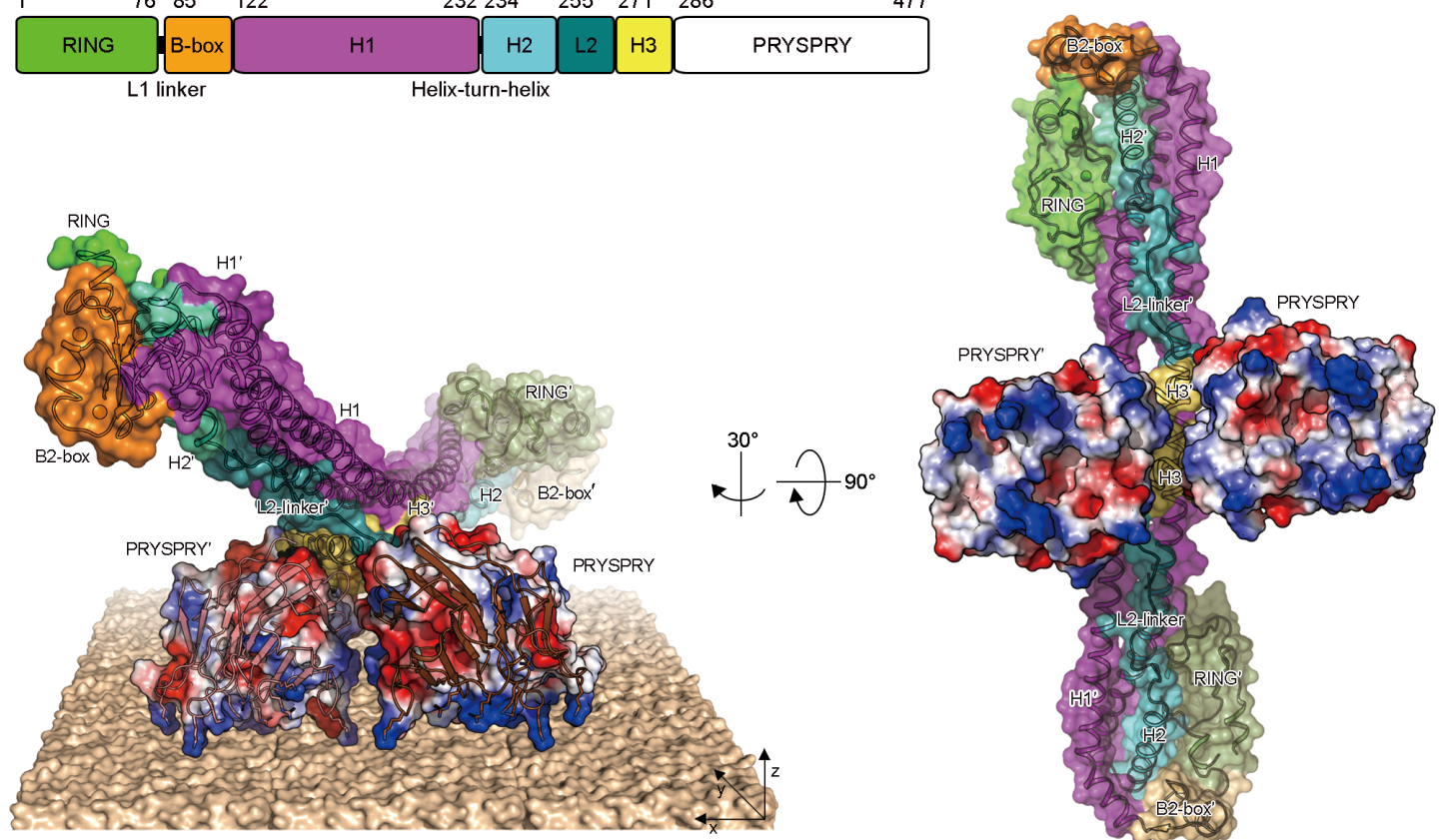


**Figure 1**

### Structure of TRIM72.

**a**, Domain organization of TRIM72. Each domain is shown as follows: RING (green), B-box (orange), H1 (magenta), H2 (cyan), L2 (teal), H3 (yellow), and PRYSPRY (white). Residues and small motifs are annotated on the top and bottom, respectively. **b**, Overall structure of TRIM72 represented by a surface and ribbon diagram. The color of each domain corresponds to the domain architecture in panel **a**. The

second protomer is labeled with a prime (') and shown in less vibrant colors. PRYSPRY domains are shown with an electrostatic potential surface (positive and negative charges shown in blue and red, respectively). Positively charged residues are represented as a stick model. The proposed membrane-binding mode of TRIM72 is also shown. The membrane model was generated from the POPS/POPC bilayer<sup>48</sup>.

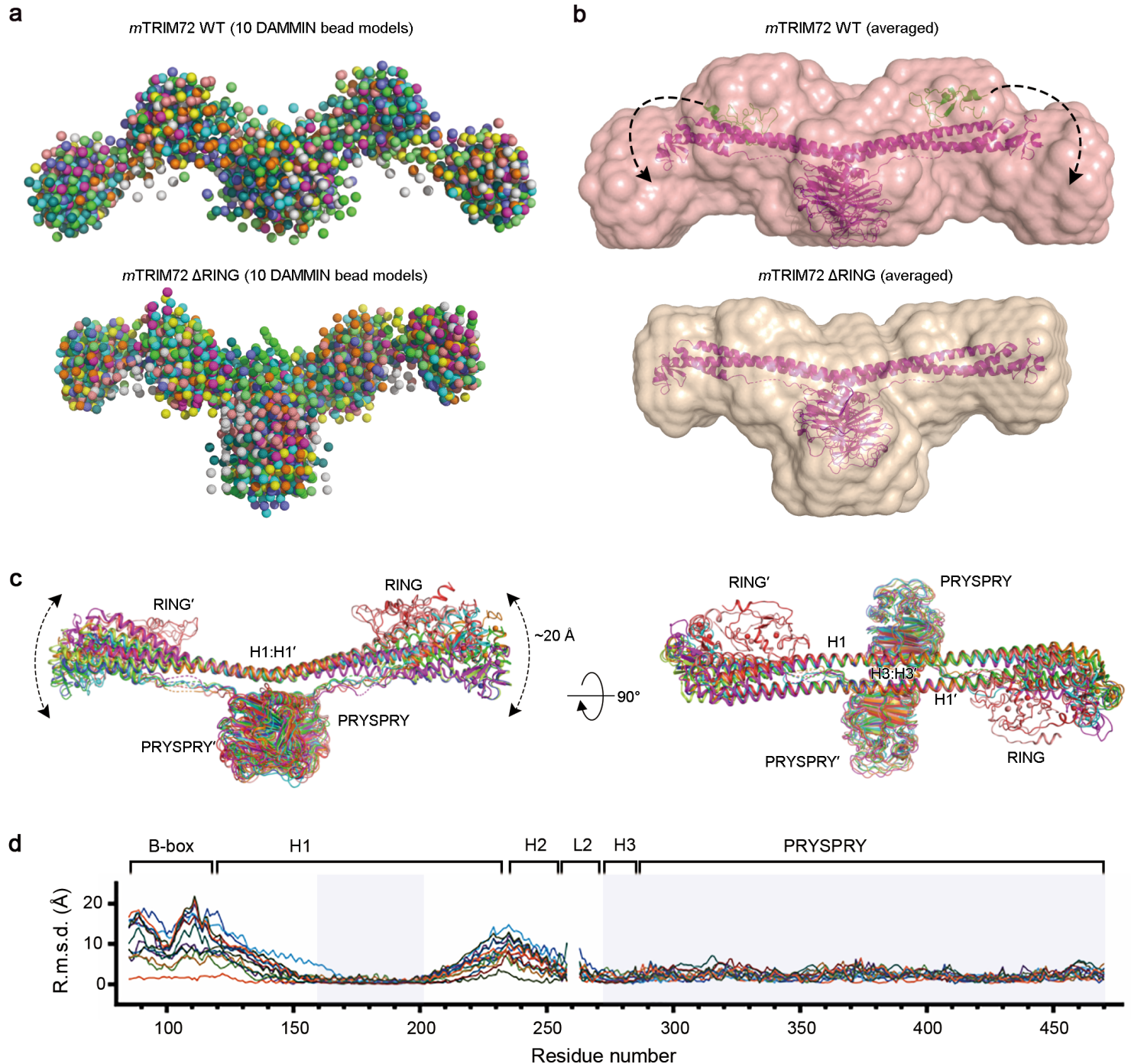


**Figure 2**

**Flexibility of the RBCC domain of TRIM72.**

**a**, *Ab initio* DAMMIN bead models of full-length TRIM72 WT (upper) and TRIM72 ΔRING (lower). Ten bead models of each protein are superimposed. **b**, Small-angle X-ray scattering molecular envelope models of TRIM72 (upper) and TRIM72 ΔRING (lower). High-resolution crystal structures of the TRIM72 ΔRING dimer (magenta) and RING (green) are superimposed and shown as ribbon diagrams. Each envelope model was generated from an average of 10 bead models in panel **a**. The additional volume at both ends of the full-length TRIM72 is expected to represent the RING domain in its position when in an open conformation in solution. **c**, Conformational movement of the coiled-coil. Superposition of all eight determined structures shows that the core formed by the central H1:H1' and H3:H3' helices and a pair of PRYSPRY domains is highly rigid, whereas the peripheral H1 and H2 helices and B-box domain are highly flexible with a maximum movement of 20 Å. Intriguingly, the coiled-coil moves in only one direction, moving closer to and farther from the membrane. **d**, Plot of the root-mean-square deviation (r.m.s.d.) of equivalent Ca atoms between full-length and various models as a function of residue number. Rigid parts are transparent cyan-colored in the Ca-r.m.s.d. plot.

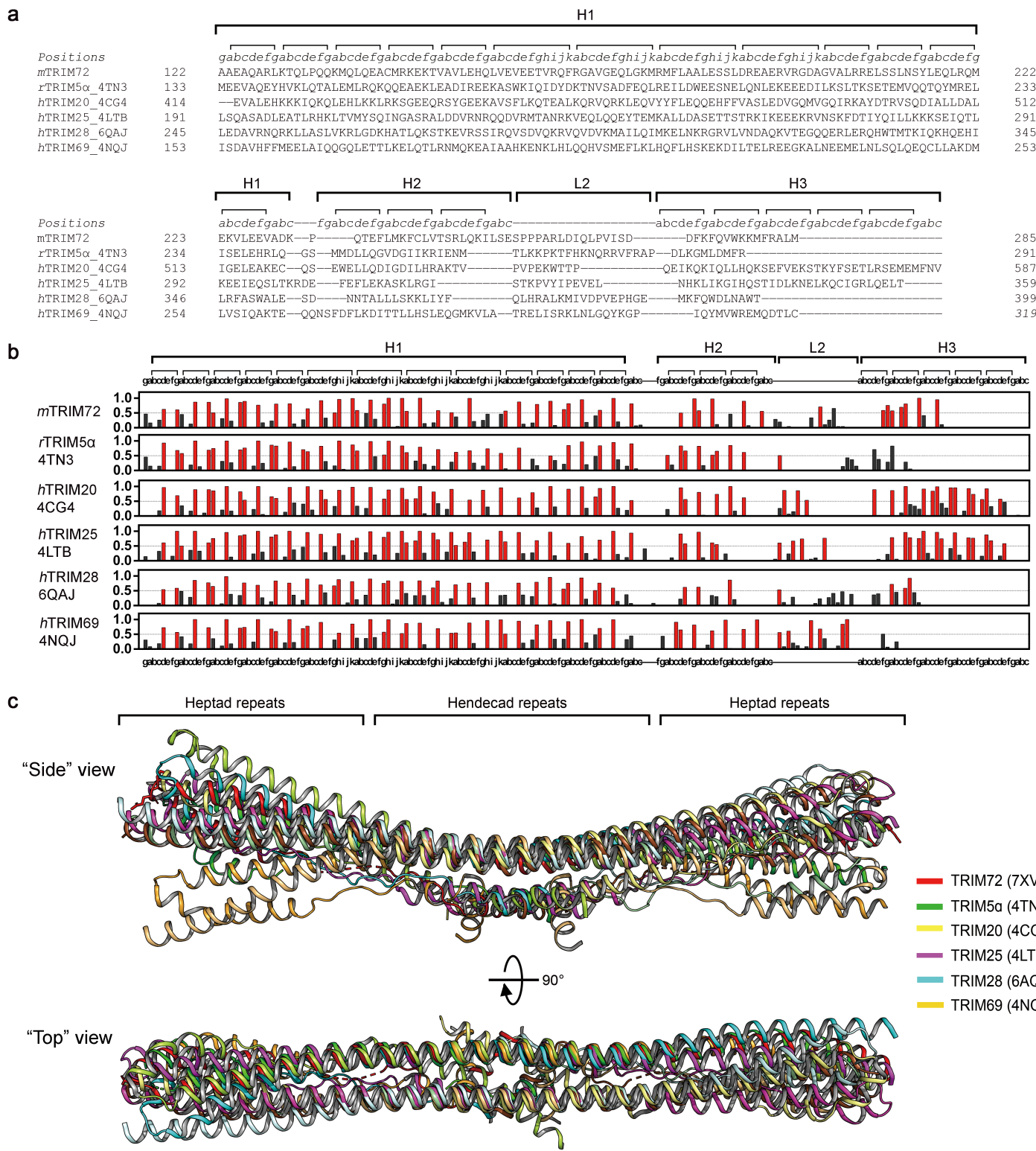


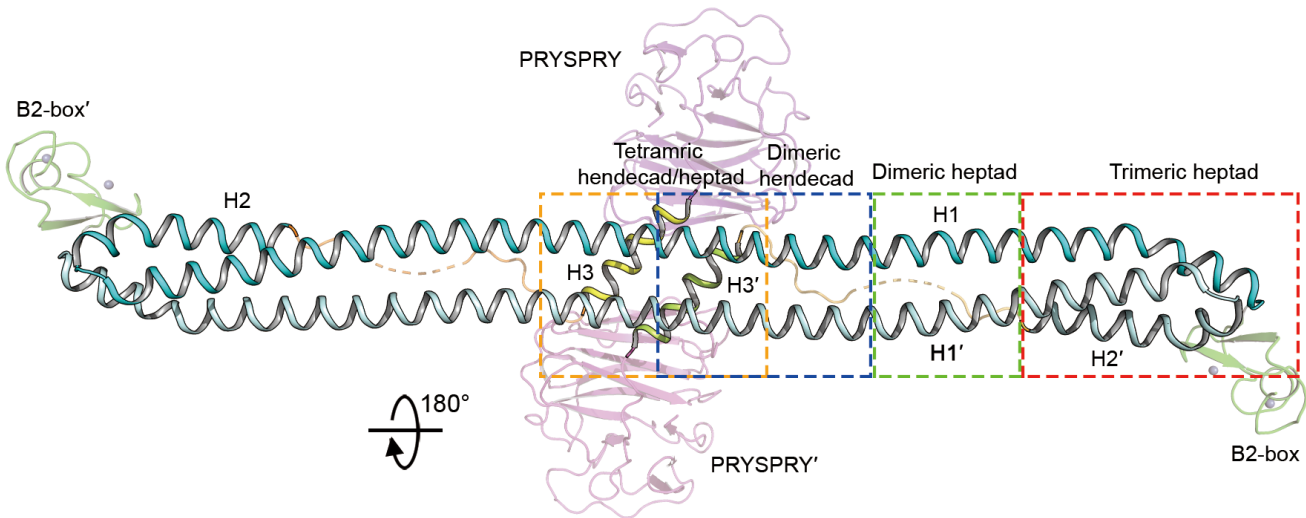
**Figure 3**

**“Up and down” motion of the TRIM coiled-coil.**

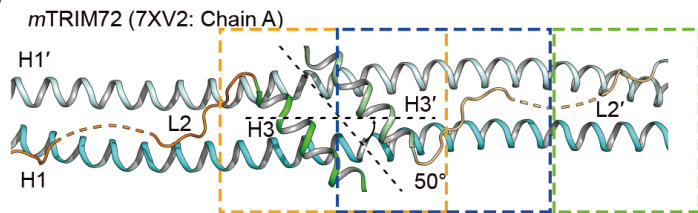
**a**, Structure-based sequence alignment of TRIM coiled-coil domains. Subdomains are annotated by thick brackets at the top (H1, H2, L2 and H3). The heptad (*a-g*) and hendecad (*a-k*) repeat positions are indicated by thin brackets above the amino acids. TRIM proteins and their PDB codes are indicated in

front of the sequences with their species (*m*, mouse; *h*, human; *r*, rhesus). **b**, Buried accessible surface area (ASA)/total ASA plots. Red bars indicate residues for which more than half of the ASA is buried within the interfaces. **c**, Superimposition of the TRIM coiled-coil. Four-hendecad helices of each dimer were aligned with the CE algorithm<sup>61</sup>. Each coiled-coil domain is shown in the ribbon diagram and colored as follows: *m*TRIM72 ΔRING, red; *r*TRIM5a, green; *h*TRIM20, yellow; *h*TRIM25, magenta; *h*TRIM28, cyan; *h*TRIM69, orange. The broad distribution of each flexible end of the TRIM coiled-coil is viewable in only the “side” view (upper) and not the “top” view (lower) obtained by a 90° rotation.

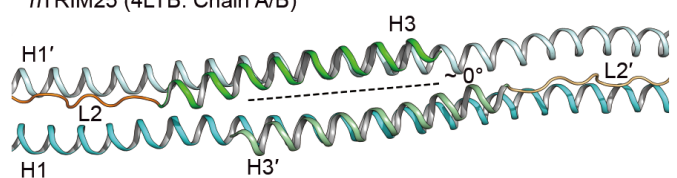
**a**



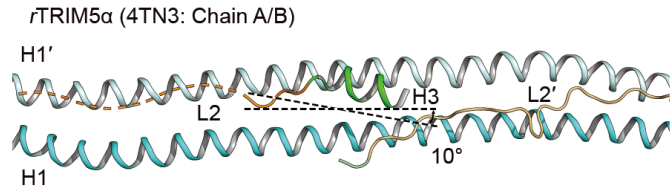
**b**



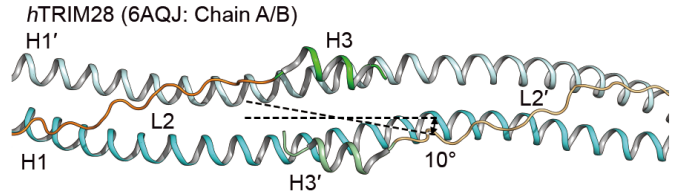
**e**



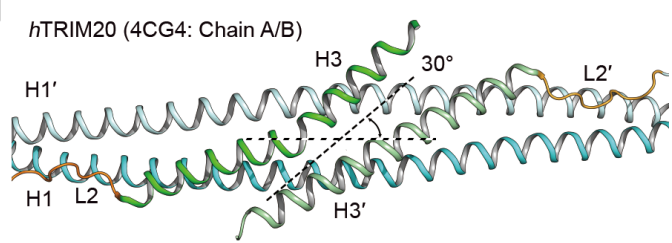
**c**



**f**



**d**



**g**

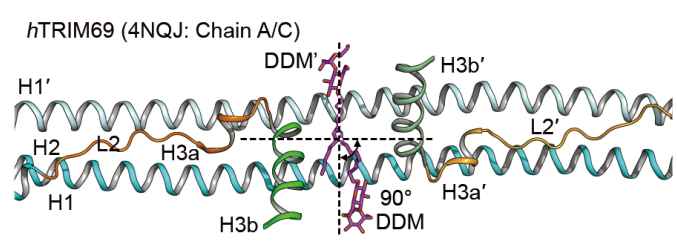


**Figure 4**

Structural comparison of the coiled-coil domain in other TRIM proteins.

**a**, Overall structure of the *mTRIM72* coiled-coil shown as a ribbon diagram. The interactions are categorized as belonging to four regions: trimeric heptad (red dashed box), dimeric heptad (green dashed box), dimeric hendecad (blue dashed box), and tetrameric hendecad/heptad (orange dashed box). **b**, Structure of the coiled-coil region of TRIM72 (PDB ID: 7XV2). The view represents the 180° rotation along the horizontal axis of panel (a) for showing the H3 and H3' helices. **c-g**, Comparison of similar regions in other TRIM proteins (**c**, *rTRIM5α*; **d**, *hTRIM20*; **e**, *hTRIM25*; **f**, *hTRIM27*; **g**, *hTRIM69*) with the tetrahelicalbundle of *mTRIM72* (orange dash boxed region of panels **a** and **b**). The H3:H3' interactions might be eliminated due to C-terminal domain deletion in the constructs (*rTRIM5α* and *hTRIM28*) or detergent binding (*hTRIM69*). The other protomer is labeled with a prime ('') symbol. The angle between central H1:H1' and H3:H3' helices are indicated **b-g**. DDM; *n*-dodecyl β-d-maltoside.

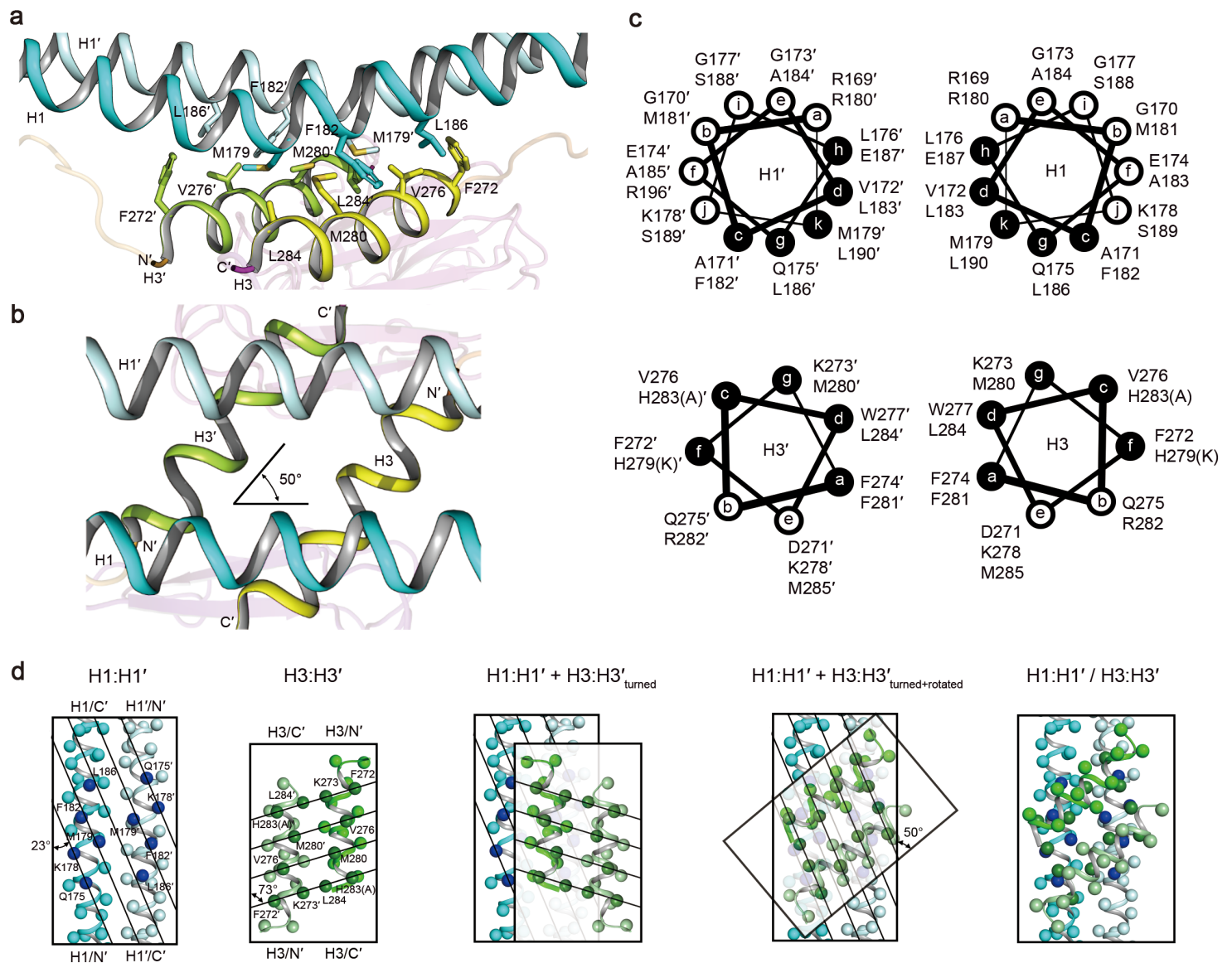
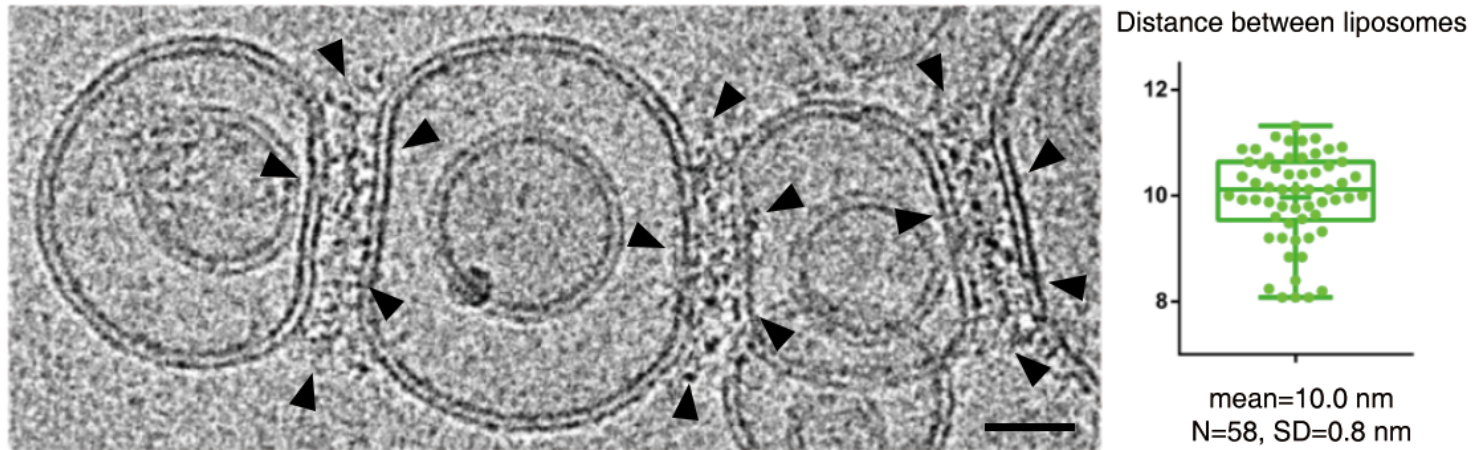


Figure 5

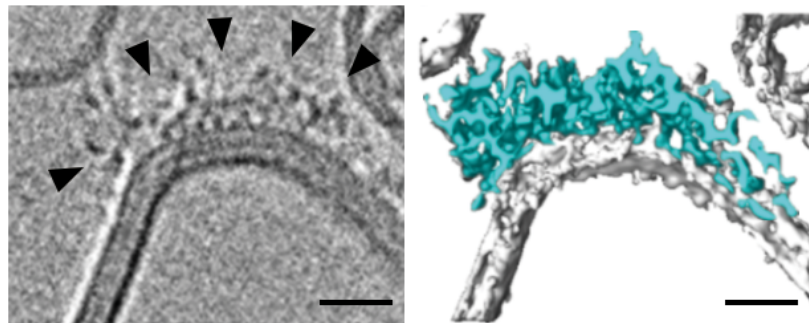
Helical bundle interaction of heptad-hendecad repeats in the TRIM72 coiled-coil.

**a**, Four-helical bundles of heptad-hendecad repeats in the orange dashed box region of **Fig. 4a** shown as ribbon diagrams. **b**, Each heptad and hendecad dimer interacts at an angle of 50°. **c**, Four-helical bundles of heptad-hendecad repeats shown as helical wheel diagrams. Black circles represent hydrophobic repeats buried in the interface. **d**, “Ridges and groove” model of the heptad-hendecad interaction. C<sub>β</sub> atoms are shown as spheres. The amino acid residues of TRIM72 are labeled. The other protomer is labeled with a prime (') symbol. For H279(K) and H283(A), residues in parentheses are from TRIM72 (**c** and **d**).

**a**



**b**



**c**

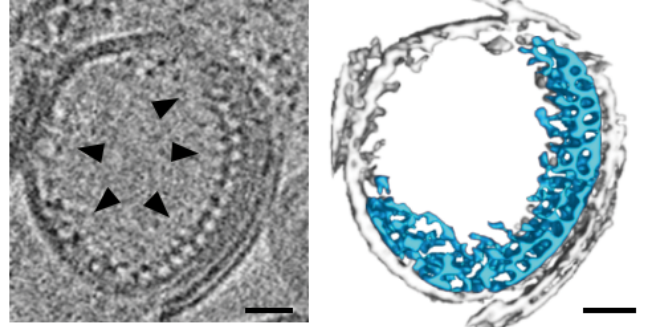


**Figure 6**

### Higher-order TRIM72 assembly on the lipid membrane.

**a**, Cryo-electron micrograph showing proteoliposomes with the TRIM72 oligomer on phosphatidylserine-SUVs. TRIM72-TRIM72 contacts were observed in the peripheral region between separate liposomes (left). Box plot of the distance between the TRIM72 oligomer-bound liposomes (right). Mean and median values (small and long bar in the box, respectively) display the first and third quartiles (upper and lower end of the box, respectively). Each individual value (dot) is represented with whiskers from minimum to maximum. **b-c**, Tomograms showing TRIM72 oligomers on the outside convex (**b**) and inside concave (**c**) surfaces of liposomes (adapted from our previous work<sup>33</sup>). Three-dimensional volume rendering (right) of each tomogram (left) with the TRIM72 oligomer and liposome shown in cyan and white, respectively. Black scale bars indicate 20 nm. Black arrowheads indicate higher-order-assembled dimeric TRIM72 molecules.

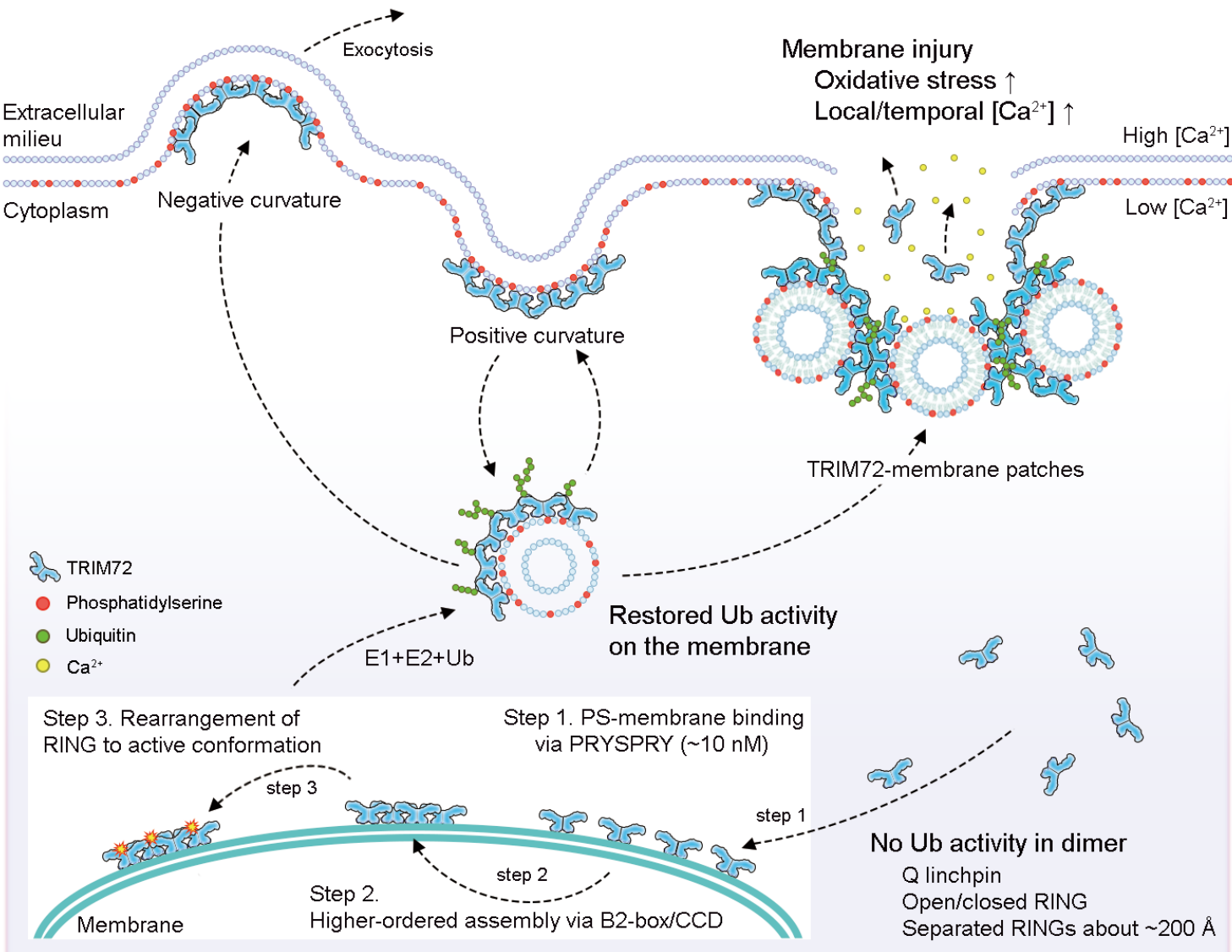


**Figure 7**

### Proposed working model of TRIM72.

The TRIM72 E3 ubiquitin (Ub) ligase is an inactive dimer in the cytosol due to dynamic changes in the RING domains with a glutamine linchpin separated by a distance of approximately 200 Å. TRIM72 is activated via three sequential molecular transitions. Using a unique pair of PRYSPRY domains, TRIM72 binds to the phosphatidylserine (PS)-enriched membrane (step 1) and forms a higher-order assembly via the B2-box and coiled-coil domains (step 2). The apparent binding affinity between the oligomer and liposome is high (approximately 10 nM) owing to avidity. Ubiquitylation activity and results of the crosslinking assays suggested that the RING domains in the oligomer rearrange to adopt an active conformation on the membrane (step 3). In the presence of E1, E2, and Ub molecules, TRIM72 catalyzes its self-ubiquitylation. Interestingly, the “up and down” motion of the wing-like coiled-coils allows interaction with both negatively and positively curved membranes. Therefore, TRIM72 proteins are present on the surface of microsomes and on both the convex and concave surface regions of the

plasma membrane. When the plasma membrane is injured, TRIM72-decorated repair vesicles are recruited to the site of damage. TRIM72 mediates the formation of membrane patches between repair vesicles and might help to bridge the plasma and vesicle membranes at damaged sites. Self- or non-self-ubiquitylation by TRIM72 might be involved in the repair machinery; however, this could not be confirmed in this study. Most likely, TRIM72-mediated repair is much faster than calcium-dependent annexin activity is<sup>62</sup>. When the calcium concentration becomes extremely high in the outer region of the plasma membrane, TRIM72 molecules bound to vesicles might dissociate and be directly secreted into the extracellular milieu. In another pathway, TRIM72, which is localized on the concave surface of the plasma membrane, might be involved in exocytosis via membrane budding.

## Supplementary Files

This is a list of supplementary files associated with this preprint. Click to download.

- [Supple.pdf](#)